LAWRENCE
LIVERMORE
NATIONAL
LABORATORY

LLNL-CONF-668393

An Experimental and Modeling Study of the Autoignition of n-Butylcyclohexane over a Wide Pressure, Temperature and Equivalence-Ratio Range

W. J. Pitz, C. Conroy, J. Bugler, H. J. Curran

March 11, 2015

9th U. S. National Combustion Meeting
Cincinnati, OH, United States
June 17, 2015 through June 20, 2015

Disclaimer

9th U. S. National Combustion Meeting
Organized by the Central States Section of the Combustion Institute
May 17-20, 2015
Cincinnati, Ohio

An Experimental and Modeling Study of the Autoignition of n-Butylcyclohexane over a Wide Pressure, Temperature and Equivalence-Ratio Range

W. J. Pitz [1], C. Conroy [2], J. Bugler [2], H. J. Curran [2]*

[1]Material Science Division, Lawrence Livermore National Laboratory, P. O. Box 808, Livermore, CA 94551 USA
[2] Combustion Chemistry Centre, National University of Ireland, Galway, Ireland
[*]Corresponding Author Email: pitz1@llnl.gov

Abstract: Chemical kinetic models of gasoline, jet, and diesel fuels and their mixtures with biofuels are needed to assess fuel effects on performance, emissions, and efficiency in practical combustion devices like internal combustion engines and gas turbine combustors. Since these fuels have too many fuel components to represent in a chemical kinetic model, surrogate fuels containing fewer components are used to represent real fuels. These surrogate fuel mixtures represent the chemical classes or the molecular structures contained in the real fuel. Alkyl cyclohexanes comprise a chemical class that is present in significant concentrations in gasoline, jet, diesel fuels and their mixtures with biofuels. Mueller et al. [Energy & Fuels 26 (6) (2012) 3284–3303] proposed n-butylcyclohexane as a component in a 9-component surrogate to represent the ignition properties, distillation curve, density, and molecular structures of two diesel reference fuels made from refinery streams. In the present work, experimental measurements of the ignition properties of n-butylcyclohexane in shock tubes and a rapid compression machine are reported over a temperature range of 630–1420K, pressures of 10, 30 and 50 atm, and equivalence ratios of 0.3, 0.5, 1.0 and 2.0 in 'air'. This wide range of conditions is considered to enable validation of a chemical kinetic mechanism for n-butylcyclohexane under conditions found in diesel engines. A detailed chemical model is developed for n-butylcyclohexane to simulate its ignition at both low and high temperatures and at elevated pressures. The experimentally measured ignition-delay times are used to improve and validate the chemical kinetic model.

Keywords: n-butylcyclohexane, shock tube, rapid compression machine, autoignition, chemical kinetic mechanism

1. Introduction

Cycloalkanes are important class of compounds in transportation fuels. In gas turbine engines for aircraft application, they absorb significant quantities of heat and remain stable [1]. For new sources of alternative fuels, like oil-sand fuels, they are a principal component and in much higher concentrations than present in conventionally-derived fossil fuels [2]. The combustion properties of cycloalkanes are unique. Their low temperature behavior is in between that of n-alkanes and olefins. They often show more low-temperature chemistry (negative temperature coefficient behavior-NTC) than olefins, but less than n-alkanes. This means that when cycloalkanes are present in gasoline or diesel fuels, they affect the ignition properties in a subtle way. At lower temperatures, cycloalkanes are consumed by reaction with radicals (such as OH). This leads to the production of unsaturated species like allylic radicals which are known to

suppress ignition chemistry. Since cycloalkanes are prevalent in gasoline, jet, and diesel fuels, the production of these allylic radicals will suppress autoignition reactions, particularly at intermediate temperatures. Proper simulation of this suppression is essential for predicting the autoignition behavior of real fuels. The sooting behavior of cycloalkanes is also interesting. Based on threshold sooting index (TSI) measurements, the sooting tendency of 2-ring cycloalkanes (e.g. decalin) is much higher than that of n-alkanes (e.g. n-decane and do-decane) [3]. Although the aromatic content mainly controls the sooting behavior real fuels, proper accounting of the sooting behavior of cycloalkanes may be necessary for accurately predicting real-fuel sooting behavior.

This paper focuses on the autoignition behavior of n-butylcyclohexane (NBCH). This particular cycloalkane was chosen because it is a component in a 9-component surrogate palette to represent real diesel fuel [4]. This 9-component palette was developed to represent the properties of real diesel fuel (e.g. California diesel certification fuel) in terms of cetane number, distillation curve, density, and chemical functional groups. Development of a validated chemical kinetic model for NBCH is needed to complete a mechanism for this diesel surrogate palette.

The previous work on NBCH is limited. Experimentally, NBCH oxidation has been studied in a flow reactor to determine its low temperature behavior [5]. They investigated its oxidation from 600 to 820 K at 0.8 MPa pressure, 0.120 s residence time, and 0.38 equivalence ratio. They observed that NBCH started to react at 615K, with a maximum reaction at 650K and with NTC behavior from 670 to 825K. Detailed species concentrations were measured at 4 temperatures spanning the temperature range. The flame speeds of NBCH were measured by Ji et al. [6] at 353, 1 atm and a range of equivalence ratios. They found NBCH to have similar flame speeds to other alkyl-cyclohexanes and that the length of the alkyl chain had a secondary effect on the flame speed. Liu et al. [7] investigated the non-premixed ignition of a series of cyclohexanes in a counterflow flame at 1 atm with ignition temperatures between 1250 and 1350K. They found that the length of the alkyl chain on the alkyl-cycloalkane had no measureable effect on ignition because of the competition between fuel reactivity and diffusivity. Hong et al. [8] measured the shock tube ignition of NBCH and the time evolution of OH and water over a temperature range of 1280 to 1480K, pressures of 1.5 and 3 atm and equivalence ratios of 0.5 and 1. They found that NBCH had similar ignition times as cyclohexane, but smaller ignition delay times than methylcyclohexane. They also measured concentration histories of OH radicals and water at early times. They found that the JetSurf version 1.1 mechanism [9] was not able to accurately reproduce the OH histories.

With respect to mechanism work, previously a detailed chemical kinetic mechanism for NBCH has been developed for high temperatures with a simplified mechanism for low temperatures [10]. This mechanism has been used to overall successfully simulate premixed laminar flame speeds, ignition in a counterflow flame, and ignition and species histories in a shock tube. However, the mechanism has a limited low temperature mechanism intended to account for some low temperature effects, but not intended for full simulation of low temperature ignition behavior. To aid in the development of improved mechanisms of NBCH, electronic structure calculations have been carried out Ali et al. [11]. They computed more accurate fuel ring-opening rate constants by using a single-reference method (quantum composite G3B3). Seven channels for ring-opening were computed. The question of whether single-reference methods are

sufficient or whether multi-reference methods are needed remains to be resolved. Ali et al. stated that previous studies have shown that the use of Gaussian-3 (single-reference) method is sufficient for mechanism development and rate constant calculations. In prior work on cyclohexane, a multi-reference method (CASPT2/cc-pVDZ) [12] was used to compute the fuel-ring opening reaction of cyclohexane directly to 1-hexene.

In this paper, new experiments are reported on the autoignition properties of n-butylcyclohexane in a shock tube and rapid compression machine. A detailed chemical mechanism for n-butylcyclohexane is developed to simulate these experiments which are used to validate the mechanism.

2. Methods / Experimental

2.1 Shock tubes

Two shock tubes were utilized in this study to acquire ignition delay times. Experimental data at reflected shock pressures of 10 and 30 atm were obtained in an intermediate-pressure shock tube. This shock tube was replaced with another, which is capable of higher pressure measurements, and was designed, fabricated, installed and validated in early 2012. This was used for the 50 atm experiments presented herein. Brief descriptions of both shock tubes will be given here. More detailed descriptions of the intermediate- and high-pressure shock tubes can be found in [13] and [14], respectively.

Ignition delay times at 10 and 30 atm were measured in an intermediate-pressure shock tube consisting of a stainless steel tube of 8.76 m in length, with an internal diameter of 6.35 cm. A double-diaphragm section divides the shock tube into a 3 m long driver section and a 5.73 m driven section. Polyethylene terephthalate films (KATCO) were used as diaphragms in all experiments, where the thickness of the diaphragm material was chosen depending on the desired final shock pressure and varied from 75–500 μm. The driver gas used was helium (99.99% pure; BOC). The diagnostic system involves four pressure transducers, where the velocity of the incident shock wave was measured at three locations separated by known distances with the shock velocity extrapolated to the endwall. The pressure at the endwall was monitored using a pressure transducer (PCB, 113A24). The incident shock velocity at the endwall was used to calculate the temperature and pressure of the mixtures behind the reflected shock wave using the equilibrium program Gaseq [15].

The ignition delay time was defined as the interval between the rise in pressure due to the arrival of the shock wave at the endwall and the maximum rate of rise of the pressure signal. Pressure traces were obtained using a Sigma digital oscilloscope (Sigma, 90–4). Any pressure profiles exhibiting significant pre-ignition pressure rise ($\geqslant$5%/ms) were excluded from the study as this has been shown to cause inaccurate measurements of ignition times in a study carried out by Shen et al. [16].

Ignition delay times were measured at 50 atm using a high-pressure shock tube. The previous intermediate-pressure shock tube was replaced so that we could perform higher pressure experiments with the operational pressure limit of the present shock tube being approximately 100 atm. The size of the present shock tube is the same as that of the previous one (8.76 m in length; 6.35 cm in the internal diameter). A double-diaphragm section divides the tube into a 3 m

long driver section and a 5.73 m driven section. Aluminum plates were used as the diaphragm material, where the thickness of the diaphragms was chosen depending on the desired final shock pressure and varied from 0.8–2.0 mm. Six pressure transducers on the sidewall (PCB; 113A24) and one at the endwall (Kistler; 603B) were used to measure the velocity of the incident shock wave, which was used to calculate the temperature of the mixtures behind the reflected shock wave using the program Gaseq [15]. Pressures behind the reflective shock wave were measured using the pressure transducer in the endwall. Pressure traces were obtained using two digital oscilloscopes (TiePie Handyscope HS4 oscilloscope). The ignition delay time was defined as the interval between the rise in pressure due to the arrival of the incident shock wave at the endwall and the maximum rate of rise of the pressure signal. The pressure rise before ignition is approximately 3%/ms in the present shock tube.

Estimated uncertainty limits of the measurements in both shock tubes are ±15 K in reflected shock temperature, T_5, ±15% in ignition delay time, τ, and ±1% in mixture concentration.

2.2 Rapid compression machine

The RCM used here is a clone of the original NUI Galway one which is characteristically different to most other RCMs in that it has a twin-opposed piston configuration as described previously [17], resulting in a fast compression time of approximately 16 ms. Additionally, creviced piston heads are used to improve the post compression temperature distribution in the combustion chamber [18]. The design for these creviced piston heads was originally devised at MIT [19] and [20], who found that the temperature field obtained using creviced pistons is almost homogeneous compared to that obtained using flat piston heads which is predicted to lead to far greater gas in-homogeneities in the post-compressed combustion chamber. A computational fluid dynamics (CFD) study carried out at NUI Galway [21] supports this view.

In our RCM it is possible to reach different compressed gas temperatures by (i) varying the diluent gas used, typically we use CO_2, N_2 or Ar, (ii) varying the compression ratio, in our case by using different sized piston heads and (iii) using different initial temperatures. We used two different sized piston heads in this study, one with a longer body such that we achieve a compression ratio of approximately 13:1 and another with a smaller body where we achieve an approximate compression ratio of 9.5:1. Using pure CO_2 as the diluent allowed us to measure ignition times at the lowest temperatures, while the use of Ar allows higher temperatures to be studied due to its lower heat capacity, while pure N_2 lies in between these two.

The reaction chamber is wrapped in double-stranded heating tape (Flexelec, 1250 W) which is insulated, and allows the variation of the initial temperature to a maximum of 140 K. By changing (i) the diluent gas composition, (ii) the piston heads and (iii) using the heating system it was possible to study a compressed gas temperature range of 630–990 K.

The heating system is also installed on the manifold and mixing tanks, to ensure that *n*-butylcyclohexane does not condense in the experiments. The manifold is heated by first attaching "type K" thermocouples at various locations along the manifold. Flexelec heating tapes are wrapped around the manifold and these were covered with Zetex 1000 insulation tape. The thermocouples were connected to both the heating tapes via a Cal 9900 thermostat and a Pico TC-08 USB thermocouple data logger (which in turn was connected to a PC). The temperatures

in the manifold were monitored to keep the reactant mixtures above the saturation temperature of *n*-butylcyclohexane at the reactant pressure at all times.

Pressure–time profiles are measured using a pressure transducer (Kistler 603B) and transferred via an amplifier (Kistler 5018) to an oscilloscope (Picoscope 4424) and ultimately recorded digitally on computer using the Picolog PC software. The non-linearity of the pressure transducer is less than ±1% of the full scale output. The ignition delay time, defined as the time from the peak pressure near the end of compression to the maximum rate of pressure rise during ignition, is measured using two vertical cursors on the oscilloscope. In general, it was found that the ignition delay times were reproducible to within 15% of one other at each compressed temperature. The compressed gas pressure was measured using two horizontal cursors.

The time for compression is fast, ≈16 ms, with most of the rapid rise in pressure and temperature taking place in the last 2–3 ms of compression; therefore heat losses during compression are small. For a period following compression, the gases experience a high degree of heat loss owing to the high temperature of the gas within the chamber relative to the chamber walls. Heat losses continue from the core gas during the constant volume period. For this reason, non-reactive pressure traces are taken to account for these heat losses in simulations of the RCM ignition experiments. These non-reactive pressure traces were obtained by replacing the oxygen content with inert nitrogen.

The compressed gas temperature, T_C, was calculated using the initial temperature, T_i, pressure, p_i and reactant composition and the experimentally measured compressed gas pressure, p_C, defined as the maximum pressure immediately after compression, and employing the adiabatic compression/expansion routine in Gaseq [15], which uses the temperature dependence of the ratio of specific heats, γ, according to the equation:

$$\ln\left(\frac{p_c}{p_i}\right) = \int_{T_i}^{T_C} \frac{\gamma}{\gamma - 1}\frac{dT}{T}$$

while assuming frozen chemistry during compression. The compressed gas temperature is then plotted against the measured ignition delay time to obtain overall reactivity profiles of *n*-butylcyclohexane.

3. Mechanism development

The NBCH mechanism was built on top of the previously developed methylcyclohexane mechanism [22], which includes the AramcoMech C0-C4 base chemistry (version 1.3) [23] and a submechanism for cyclohexane. The methylcyclohexane has recent updates on its low temperature chemistry [22] and analogous reaction rates are used for NBCH.

For the high temperature chemistry, the reaction classes below are included:

High Temperature Reaction Classes
1. Unimolecular fuel decomposition
2. H-atom abstraction from the fuel
3. Alkyl radical decomposition

4. Alkyl radical isomerization
5. H-atom abstraction reactions from alkenes
6. Addition of radical species O and OH to alkenes
7. Reactions of alkenyl radicals with HO_2, CH_3O_2, and $C_2H_5O_2$
8. Alkenyl radical decomposition
9. Alkene decomposition
10. Retroene decomposition reactions

For Reaction Class 1, the recent fuel decomposition rates computed by Ali et al. [11] are adopted. For the rates of H-atom abstraction from the fuel (Reaction Class 2), no measurements or quantum chemistry calculations have been made for NBCH and the acyclic reaction rate rules from Sarathy et al. [24] are used. These acyclic rates are close to cyclic rates that have been measured. For example for NBCH + OH, the rate of secondary abstraction on the ring computed by Sivaramakrishnan and Michael [25] for MCH is within 20% of the acyclic rate from Sarathy et al. For the decomposition of NBCH radicals (Reaction Class 3), rate constants from JetSurf 2.0 are adopted [10]. These rate constants are pressure-dependent, 9-parameter (Troe) fits. Based on the notes in JetSurf 2.0, these rate constants are based on acyclic rate constants from the published work and work-in-progress of Tsang and coworkers, e.g. [26]. For the NBCH radical isomerizations (Reaction Class 4), the rate constants are mostly estimated by Sirjean and Wang as in JetSurf 2.0. For the isomerizations on the alkyl group only, the isomerization rates are from Sarathy et al. [24]. Concerning the chemistry of the cyclic alkenes formed from NBCH, all the butylcyclohexene isomers are included. The rate of abstraction of H atoms (Reaction Class 5) is based on all the easily abstractable H-atoms in these cyclic alkenes. However, the cyclic alkenyl radicals are lumped into the resonantly stabilized form because these are the most likely to be formed. This assumption also reduces the size and complexity of the mechanism. The Waddington mechanism [27] (included in Reaction Class 6) is included for the cyclic alkenes because these reactions can be important in enhancing OH production. For other high temperature reaction classes, the reader is referred to the well-annotated mechanism which gives the pedigree of each reaction rate constant. The mechanism will be made available upon literature publication of this work.

For the low temperature chemistry, the following reaction classes were included:

Low Temperature Reaction Classes

11. Addition of O_2 to alkyl radicals (R + O_2 = ROO)
12. R + ROO = RO + RO
13. R + HO_2 = RO + OH
14. R + $CH3O_2$ = RO + CH_3O
15. Alkyl peroxy radical isomerization (ROO = QOOH)
16. Concerted eliminations (ROO = alkene + HO_2)
17. ROO + HO_2 = ROOH + OH
18. ROO + H_2O_2 = ROOH + HO_2
19. ROO + CH_3O2 = RO + CH_3O + O_2
20. ROO + ROO = RO + RO + O_2
21. ROOH = RO + OH
22. RO decomposition

23. QOOH = cyclic ether + OH (cyclic ether formation via cyclisation of diradical)
24. QOOH = alkene + HO_2 (radical site beta to OOH group)
25. QOOH = alkene + carbonyl + OH (radical site gamma to OOH group)
26. Addition of O_2 to QOOH (QOOH + O_2 = OOQOOH)
27. Isomerization of OOQOOH and formation of carbonylhydroperoxide and OH
28. Decomposition of carbonylhydroperoxide to form oxygenated radical species and OH
29. Cyclic ether reactions with OH and HO_2
30. Decomposition of large carbonyl species and carbonyl radicals

For addition of NBCH radicals to O_2 (Reaction Class 11), the rate constants from Fernandes et al. [28] for cyclohexane are used for radical sites on the ring and for radical sites on the alkyl group, acyclic rate constants recommended by Bugler et al. [29] are used who took them from Miyoshi [30]. Bugler et al. has recently developed a set of low-temperature chemistry rate constants that work well for C5 and C6 n-alkanes and iso-alkanes when comparing simulations to experiments of low-temperature ignition in rapid compression machines (RCM) and shock tubes. Similarly, for the RO_2 isomerization rate constants, isomerizations on the ring are taken from Fernandes et al. [28] and isomerization on the alkyl group are taken from the recommendations of Bugler et al. [29] who used rates from Sharma et al. [31]. For isomerizations between sites on the ring and sites on the alkyl group, rate constants from Sharma et al. are used. Originally, the rate constants from Sarathy et al. [24] were used instead of those recommended by Bugler et al. for the isomerizations on the alkyl group and between the alkyl group and the ring. This resulted in ignition delay times that were too slow compared to experiments in the shock tube and RCM. Adoption of the new recommendations from Bugler et al. resulted in a significant decrease in ignition delay times and much better agreement with the experiments. For Reaction classes 26 and 27, analogous reaction rates were adopted to Reaction Classes 11 and 15. For Reaction class 26, the recommendations from Bugler et al. were used for the alkyl sites which were based on Miyoshi [30]. These pre-exponential factors for Miyoshi were reduced by about a factor of 2 following Bugler et al. to obtain better agreement with the validation set. For the rate constant selection of the other reaction classes, the reader is directed to the well-annotated mechanism which gives the reaction rate constant pedigree for each reaction rate constant.

The rate constants in the mechanism were analyzed by a mechanism tool developed by McNenly [32] that identifies reaction rate constants which exceed theoretical limits, such as collision limits for bimolecular reactions and plausible limits for unimolecular reactions over the temperature range encountered in combustion. The reactions that exceeded these limits were identified, and these rate constants were evaluated and fixed.

The thermodynamic parameters for the species are very important because they are used to determine reverse rate constants. The C1–C4 species thermodynamic parameters were taken from Metcalfe et al. [23]. The THERM software was used to compute the thermochemical properties of NBCH-related species. Group values were taken from J.W. Bozzelli [33].

4. Results and Discussion

The results of the shock tube experiments and simulations are shown in Fig. 1 for equivalence ratios of 0.3, 0.5, 1.0 and 2.0 in ‘air’, temperatures from 670 to 1350K and pressures of 10, 30 and 50 atm. The symbols represent the experimental data and the curves the simulations. The

experimental results show that NBCH has NTC behavior in the low temperature region for pressures of 30 and 50 atm at equivalence ratios (ϕ) of 0.5, 1.0, and 2.0. At ϕ = 0.3, a nearly zero slope in the NTC region seen. Computed results using the NBCH mechanism show nearly the same behavior. Both the experimental and computed results show that the influence of pressure increases with equivalence ratio and more pressure effect is observed at lower temperatures (700 to 900 K). The simulated ignition delay times are most affected by a change in pressure from 10 to 30 atm at the temperature region below 1000K. The effect of equivalence ratio (ϕ) is most evident when ϕ is increased from 0.5 to 1 for the 30 and 50 atm cases.

The experimentally measured ignition delay times in the RCM are compared to the computed times in Fig. 2 for ϕ = 0.3, 0.5, 1.0 and 2.0 and pressures of 10 and 30 atm. In the calculations, volume histories were used to simulate the effect of compression and heat loss after the end of compression. Both the experiments and calculations showed a decrease in ignition delay time with increasing pressure from 10 to 30 atm and with increasing equivalence ratio from ϕ = 0.3 to 1.0. NTC behavior was observed in the experiments at 10 atm and ϕ = 0.5 and 1.0. The simulations matched the experimental results reasonably well at ϕ = 1.0 and 2.0. However, the simulated ignition delay times exceeded the experimental values at ϕ = 0.3 for both pressures and at ϕ = 0.5 for 10 atm.

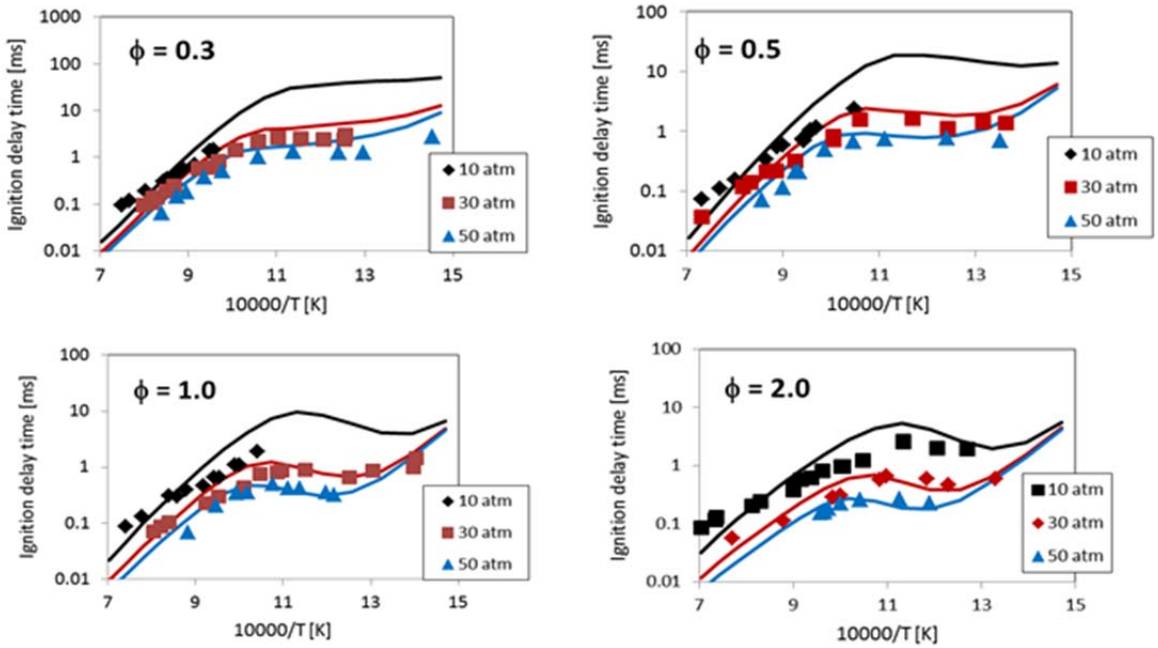

Figure 1. Experimental ignition delay times (symbols) compared to those computed using the NBCH mechanism (curves) for shock tube ignition for 4 equivalence ratios over a range of temperature and pressure.

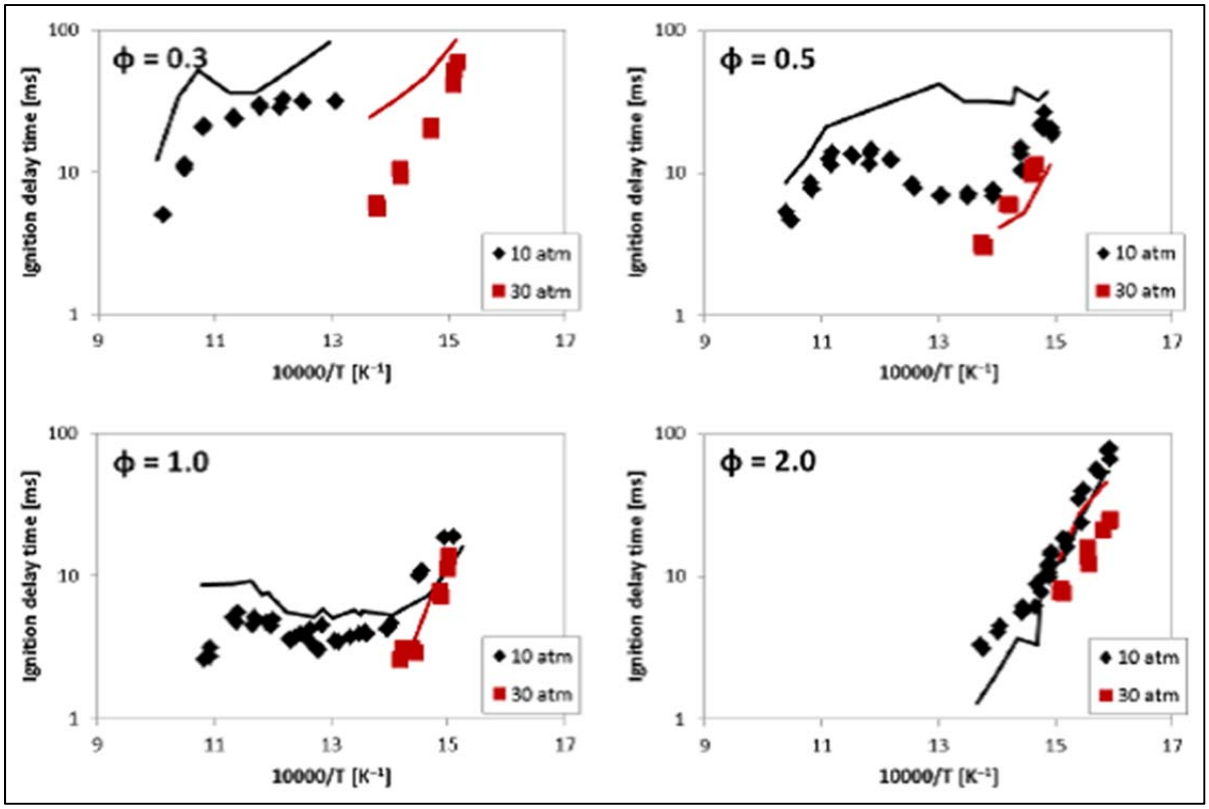

Figure 2. Experimental ignition delay times (symbols) in the RCM compared to those computed using the NBCH mechanism (curves) for 4 equivalence ratios over a range of temperature and pressure.

5. Conclusions

Ignition delay times for NBCH were measured in shock tubes and an RCM over a range of temperatures from 630 to 1420 K, pressures of 10, 30, and 50 atm and equivalence ratios of 0.3, 0.5, 1.0, and 2.0. A detailed chemical kinetic model for NBCH was developed based on the previous ones developed for methylcyclohexane and cyclohexane. The new experimental data was used to validate the chemical kinetic mechanism. It was found that more recent RO_2 isomerization rates based on ab initio calculations provided better simulations of experimental data than previously used ones from Sarathy et al. [24] that were semi-empirically based.

6. Acknowledgements

The work at LLNL was supported by the U.S. Department of Energy, Vehicle Technologies Office (program managers Gurpreet Singh and Leo Breton) and performed under the auspices of the U.S. Department of Energy by Lawrence Livermore National Laboratory under Contract DE-AC52-07NA27344.

NUIG acknowledge the financial support of Saudi Aramco and the Irish Research Council.

7. References

1. L. Turker, S. Varis, Propellants Explosives Pyrotechnics 39 (2) (2014) 211-216.

2. W. S. Neill, W. L. Chippior, J. Cooley, M. Doma, C. Fairbridge, R. Falkiner, R. L. McCormick, K. Mitchell, *Emissions from Heavy-Duty Diesel Engine with EGR using Fuels Derived from Oil Sands and Conventional Crude*, SAE 2003-01-3144, Society of Automotive Engineers, 2003.
3. A. Mensch, R. J. Santoro, T. A. Litzinger, S. Y. Lee, Combust. Flame 157 (6) (2010) 1097-1105.
4. C. J. Mueller, W. J. Cannella, T. J. Bruno, B. Bunting, H. D. Dettman, J. A. Franz, M. L. Huber, M. Natarajan, W. J. Pitz, M. A. Ratcliff, K. Wright, Energy & Fuels 26 (6) (2012) 3284–3303.
5. R. H. Natelson, M. S. Kurman, N. P. Cernansky, D. L. Miller, Combust. Flame 158 (12) (2011) 2325-2337.
6. C. Ji, E. Dames, B. Sirjean, H. Wang, F. N. Egolfopoulos, Proc. Combust. Inst. 33 (1) (2011) 971-978.
7. N. Liu, C. Ji, F. N. Egolfopoulos, Proc. Combust. Inst. 34 (2013) 873-880.
8. Z. Hong, K.-Y. Lam, D. F. Davidson, R. K. Hanson, Combust. Flame 158 (8) (2011) 1456-1468.
9. E. D. B. Sirjean, D.A. Sheen, F.N. Egolfopoulos, H. Wang, D.F. Davidson,, H. P. R.K. Hanson, C.T. Bowman, C.K. Law, W. Tsang, N.P. Cernansky,, A. V. D.L. Miller, R.P. Lindstedt A high-temperature chemical kinetic model of n-alkane, cyclohexane, and methyl-, ethyl-, n-propyl and n-butylcyclohexaneoxidation at high temperatures, JetSurF version 1.1. http://melchior.usc.edu/JetSurF/JetSurF1.1 (September 15, 2010)
10. H. Wang, E. Dames, B. Sirjean, D. A. Sheen, R. Tangko, A. Violi, J. Y. W. Lai, F. N. Egolfopoulos, D. F. Davidson, R. K. Hanson, C. T. Bowman, C. K. Law, W. Tsang, N. P. Cernansky, D. L. Miller, R. P. Lindstedt A high-temperature chemical kinetic model of n-alkane (up to n-dodecane), cyclohexane, and methyl-, ethyl-, n-propyl and n-butyl-cyclohexane oxidation at high temperatures, JetSurF version 2.0, September 19, 2010. http://web.stanford.edu/group/haiwanglab/JetSurF/JetSurF2.0/ (1/30/2013)
11. M. A. Ali, V. T. Dillstrom, J. Y. W. Lai, A. Violi, J. Phys. Chem. A 118 (6) (2014) 1067-1076.
12. J. H. Kiefer, K. S. Gupte, L. B. Harding, S. J. Klippenstein, The Journal of Physical Chemistry A 113 (48) (2009) 13570-13583.
13. D. Darcy, C. J. Tobin, K. Yasunaga, J. M. Simmie, J. Wuermel, W. K. Metcalfe, T. Niass, S. S. Ahmed, C. K. Westbrook, H. J. Curran, Combust. Flame 159 (7) (2012) 2219-2232.
14. H. Nakamura, D. Darcy, M. Mehl, C. J. Tobin, W. K. Metcalfe, W. J. Pitz, C. K. Westbrook, H. J. Curran, Combust. Flame 161 (1) (2014) 49-64.
15. C. Morley, *GasEq*, Version 0.76, http://www.gaseq.co.uk, 2004.
16. H.-P. S. Shen, J. Vanderover, M. A. Oehlschlaeger, Proc. Combust. Inst. 32 (1) (2009) 165-172.
17. W. S. Affleck, A. Thomas, Proc. Inst. Mech. Eng. 183 (1969) 365–385.
18. L. Brett, J. MacNamara, P. Musch, J. M. Simmie, Combust. Flame 124 (2001) 326–329.
19. D. Lee, S. Hochgreb, Combust. Flame 114 (3-4) (1998) 531-545.
20. D. Lee, S. Hochgreb, Int. J. Chem. Kinet. 30 (6) (1998) 385-406.
21. J. Würmel, J. M. Simmie, Combust. Flame 141 (4) (2005) 417-430.
22. B. W. Weber, W. J. Pitz, M. Mehl, E. J. Silke, A. C. Davis, C.-J. Sung, Combust. Flame 161 (8) (2014) 1972–1983.
23. W. K. Metcalfe, S. M. Burke, S. S. Ahmed, H. J. Curran, Int. J. Chem. Kinet. 45 (10) (2013) 638-675.
24. S. M. Sarathy, C. K. Westbrook, M. Mehl, W. J. Pitz, C. Togbe, P. Dagaut, H. Wang, M. A. Oehlschlaeger, U. Niemann, K. Seshadri, P. S. Veloo, C. Ji, F. N. Egolfopoulos, T. Lu, Combust. Flame 158 (12) (2011) 2338-2357.
25. R. Sivaramakrishnan, J. V. Michael, Combust. Flame 156 (5) (2009) 1126-1134.
26. W. S. McGivern, I. A. Awan, W. Tsang, J. A. Manion, J. Phys. Chem. A 112 (30) (2008) 6908-6917.
27. M. S. Stark, D. J. Waddington, Int. J. Chem. Kinet. 27 (2) (1995) 123-151.
28. R. X. Fernandes, J. Zador, L. E. Jusinski, J. A. Miller, C. A. Taatjes, Physical Chemistry Chemical Physics 11 (9) (2009) 1320-1327.
29. J. Bugler, K. P. Somers, E. J. Silke, H. J. Curran, J. Phys. Chem. A (2015) submitted for publication.
30. A. Miyoshi, Int. J. Chem. Kinet. 44 (1) (2012) 59-74.
31. S. Sharma, S. Raman, W. H. Green, The Journal of Physical Chemistry A 114 (18) (2010) 5689-5701.
32. M. McNenly, in: Personal communication ed.; 2014.
33. J. W. Bozzelli, in: 2001.